Transducer Development for Nonintrusive Load Monitoring of Rotating Machinery

Mateja Putic, Nathan K. Brown, and Paul Muskopf

Luna Innovations Incorporated, Charlottesville, VA, 22903, USA
{puticm, nbrown, muskopfp}@lunainnovations.com

ABSTRACT

Monitoring machine runtime health parameters through nonintrusive means can greatly reduce the up-front time and resource barriers to entry of adding instrumentation to existing plant infrastructure. This work presents the design and evaluation of three transducers as part of a nonintrusive load monitoring system for rotating machinery. Data collected using a custom designed, small-scale induction motor test stand shows the dependence of a large air core RF coil, small RF coil array, and Hall effect sensor outputs on applied motor speeds and mechanical loads (estimated based on generator power). Analysis indicates that the large air core RF coil transducer and the presented method for using nonintrusive collection of induction motor speed and stray flux can statistically measure the difference between any two load points with 95% confidence, if their values differ by 6.6% full scale or greater ($\pm 2\sigma$). Additionally, areas of further research toward generalization of the approach are identified.

1. INTRODUCTION

Knowing the load profile of rotating machinery is an integral part of determining the useful life of motors and for predicting when motor parts will break down, and for developing maintenance schedules. While many models exist for PHM modeling of motors, the instrumentation that is necessary to collect data to feed into those models can be cumbersome to install and may require machine downtime and skilled technicians to install. Fully capable PHM system installation is especially expensive if it requires motor downtime, but in cases when the application is mission critical, downtime is not feasible. Consequently, facilities may forego the use of PHM systems completely due to the complexity of the install, leaving the benefits of these approaches as yet unrealized.

While hour meters or odometers are widely used, they do not provide indications of when the instrumented machine ran, for how long, or at what load level. For example, a machine may have a low hour count but be highly stressed if much of that time was accumulated over short run cycles. Direct methods of observing motor load include measuring output power by shaft displacement or input power by voltage, current, and power factor. Such approaches require some form of invasive instrumentation, however, such as proximity probes, torque-sensing couplings, and voltage/current interconnections, all of which are non-trivial to install, and usually constitute permanently installed instrumentation. Low-cost, non-invasive methods were desired for the present effort to ease integration effort and permit deployment on a wide range of assets.

Nonintrusive load monitoring of rotating machinery can offer a middle ground between traditional schedule-based maintenance, and fully modern PHM systems. This approach makes available an effective albeit simple indicator as a proxy for the mechanical output power of the motor. Ambient energy emitted by machinery can be tracked, analyzed, and classified to develop a motor load profile that illustrates how long a machine has run and at which load level as a percent of full scale. This type of profile can also be used to determine whether machines are operated within specifications. Finally, load profiling across a fleet of machines can be used to determine whether machine capacity is effectively distributed among plant loads, and to assist in scheduling plant capacity among parallel applications.

In related efforts on stray flux sensing, Adam, Gulez, and Koroglu (2001) provide a strong background on sensing stray flux distributions around electric motors with the objective of "provid[ing] safety regions for humans in the vicinity of these motors". This study documents methods of determining stray flux using x-axis, y-axis, and z-axis air coils mounted to the exterior of the test motor. Results from this paper provide general application rules for stray flux measurement, and this finding directed the placement of our prototype search coil on the test stand motor. An application

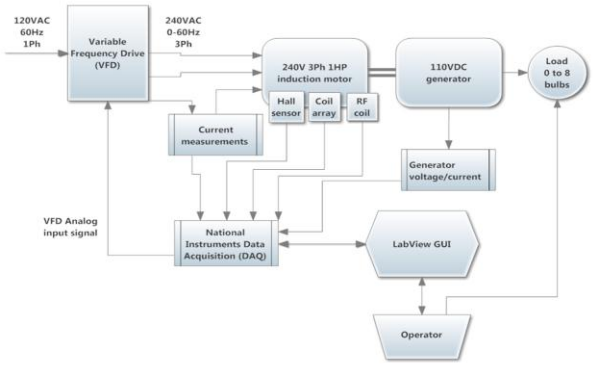

Figure 1. Motor test stand overview, instrumented for measurement of input power and output stray flux

note from the DOE Motor Challenge program (DOE, n.d.) documents traditional methods of determining motor loading and efficiency, input power or line current measurement, and a method based on slip. Additionally, Tumanski (2007) is an excellent reference for air core RF coil transducer and analog front end electronics design. Bin Lu, Habetler, and Harley (2006) provide descriptions of more than 20 efficiency estimation methods for in-service induction motors, and document the required tests and measurements, intrusion level, and average accuracy.

Our research sought to create a solution that is substantially easier to install than alternative approaches, to lower the up-front time and resource barriers to entry toward understanding plant capacity distribution. The broad vision of this system is to collect start/stop times and load levels on a widely distributed set of plant machinery, so that plant maintainers can effectively schedule maintenance resources and determine where machine capacity is underused or overused. The system presented is also designed to be compatible with energy harvesting from a variety of available sources which are abundant in the plant environment, identifying low power requirements as a factor of interest. The scope of this study details the research and development of a transducer that can reliably be used to estimate load nonintrusively through the monitoring of ambient emitted machine energy. Section 2 describes the motor test platform that was built for this study, and the design and preliminary evaluation of stray flux transducers. Section 3 details the characterization of transducer outputs over versus motor operating parameters, and describes the development of stray flux characterization models. Section 4 provides an analysis and statistical evaluation of experimental results. Section 5 contains conclusions and opportunities for further research.

2. MOTOR PLATFORM AND TRANSDUCERS

The central parameter of interest to be measured nonintrusively within this study was real-time mechanical load on an induction motor. As part of system development, several different transducers for detecting stray flux were selected for evaluation to determine the most reliable method. Initially, a motor test stand was built with controllable shaft speed and mechanical load, to facilitate evaluation of experimental transducers.

2.1. Motor Test Stand

A motor test stand diagrammed in Figure 1 was built and was used as a basis for transducer evaluations. This stand consists of a variable frequency drive (VFD), a 1 HP 240 VAC three phase AC induction motor, a 110 VDC generator mechanically coupled to the drive motor shaft, and a switchable resistive load bank of eight light bulbs. The VFD accepts an input of single phase 120 VAC and converts it to a 240 VAC three phase output. By using the VFD, speed of the motor was controlled by varying the three phase output frequency.

To correlate stray flux transducer output to motor load, a motor power estimate was obtained by measuring the output voltage and current from the DC generator. Although this approach does not take into account motor losses, generator efficiency, and frictional losses, it achieved sufficient accuracy of relative motor load for transducer characterization.

The test stand was instrumented to control motor drive speed and electrical load, measure input power, and to measure outputs from three different sensors, all simultaneously. Two Tamura L10Z050S05 Hall effect sensors that output a voltage proportional to the current flowing through the center of the sensor enabled acquisition of the current from one phase of the VFD output, as well as the current produced by the generator. The actual output frequency from the VFD was obtained through tonal analysis of the signal from the Tamura Hall effect sensor, implemented using National Instruments LabVIEW. Furthermore, the frequency of the voltage output from any installed stray flux transducers was also analyzed to verify if those measurements agree with the tone analysis of the motor current sensor voltage. These signals, as well as the voltage output from the generator, were connected to a National Instruments Multifunction Data Acquisition (DAQ) platform, which was used to directly sample these signals and import them into a LabVIEW development environment.

To provide a visual display of data and a control interface to the VFD and the DAQ, a GUI was also developed using LabVIEW. This interface allows automatic control of the VFD output frequency, load level prompting, signal acquisition and processing, and data logging, for semi-automated automated stimulus and test data collection.

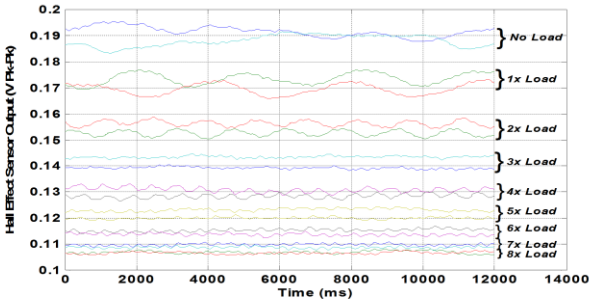

Figure 2. Hall Effect sensor amplitude for varying motor loads

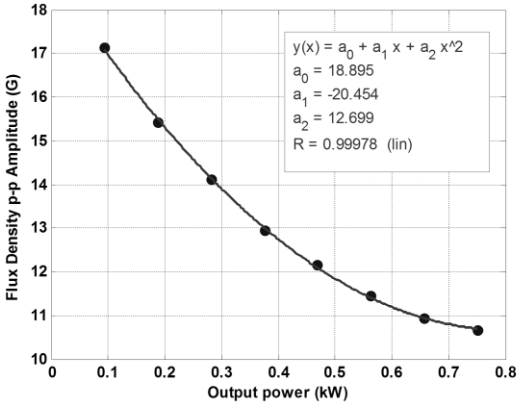

Figure 3. Relationship between RMS Hall effect sensor output and motor load

2.2. Transducer Selection

The technique employed for nonintrusive load monitoring is to utilize the stray magnetic flux emitted from the motor to infer its output power. This approach relies on the fact that the finite permeability of a motor's magnetic core cannot fully contain the generated flux from the windings, and a small portion of the core flux will ultimately stray to the surrounding environment. Although significantly reduced in scale, the stray flux density correlates with the magnitude of the motor core flux density, which is in turn a function of motor output power. Therefore, measuring stray flux density can provide an indirect, but reliable means of estimating of mechanical motor load. The following section details evaluation of a COTS Hall effect sensor, a small air core RF coil array, and large air core RF coil transducers for this purpose.

2.2.1. COTS Hall Effect Sensor

Hall effect sensors are predominantly employed to measure magnetic flux density for a variety of applications. For the present effort, the Allegro A1395 low-power linear Hall effect sensor IC was selected due to its small form factor, high sensitivity (10 mV/Gauss), and low power requirements. An initial survey of the test motor's external magnetic field distribution was performed to determine a suitable location to mount the Hall effect sensor for load monitoring. The highest response was achieved at the edge of the stator core stack, above the endturn windings.

With the Hall effect sensor in place, the stray flux density was characterized over a range of applied motor load at a constant operating speed. For each load level, recorded flux density readings display a typical AC waveform at operating frequency. The peak-to-peak amplitude of this stray flux signal is plotted for each motor load level in Figure 2 while stepping through loading and unloading cycles. For each motor load, the signal falls within a discernible voltage band, the amplitude of which decreases steadily as motor power increases. Given the rated 10 mV/Gauss sensitivity level of this transducer, the stray flux amplitudes range between 10 and 20 Gauss, or around 0.1% of the internal 10 kG flux density level within the motor.

Interestingly, the low frequency carrier wave of these peak-to-peak ripples is related to the motor power as well, likely due to the increasing rotor slip speed with increasing torque, as the induction motor rotor spins slightly slower than the alternating stator field with increasing mechanical load. The difference in rotational speed inducing current in the rotor conductors generate the corresponding torque. The low frequency ripple in these signals is established as a beat frequency between the non-identical induction rotor and stator field rotation speeds. However, this beat frequency was detectable only at low load levels, making it difficult to use this parameter as an additional indicator of machine load.

Figure 3 shows the average field amplitudes plotted against the power load level, which reveals a clear trend in both loading and unloading directions. For an induction motor, increased torque is produced by increasing rotor conductor current, resulting in a lower net current in the 'transformer' loop and consequently lower core flux. The unloaded condition is analogous to a transformer with an open secondary winding (i.e. high core flux), whereas the maximum power case represents the impedance matched condition for the transformer with good coupling between the windings, such that the core flux is considerably lower. The reduction of stray flux density with increasing motor load observed here is the expected result.

The observed repeatable trend of the Hall effect sensor output correlated with mechanical motor load demonstrates the ability of this sensor to nonintrusively monitor motor load level. Calibration in a field application would be required, following a similar surveying procedure as in this study. A calibration curve could be generated by exercising the motor of the operating range of interest while monitoring the output of the sensor. An important caveat here is that this calibration between monitored flux and

motor power will provide a reliable indication of motor load only if the sensor remains in the same mounting location.

2.2.2. Small Air Core RF Coil Array

The second transducer chosen for this effort was made up of an array of antennas salvaged from COTS RFID tags. The antenna on these tags is a small air core inductor made of 30 gauge wire with 25 mm OD and 15 mm ID and 1 mm thickness. As a preliminary survey step, a single inductive coil was adhered to the motor casing and its output RMS voltage was read with the DAQ. A clear step change was seen with each change in motor load. To increase the voltage response and measurement area, six of these coils were wired in series and bound together side by side. Though the absolute voltage output does differ with coil circumferential position, longitudinal position, distance from the coil to the motor case, and orientation, the relative voltage response to change in load did not change considerably.

2.2.3. Large Air Core RF Coil

Background research led to the choice of a single large air core RF coil as a potentially useful transducer for measuring stray flux around a motor. The RF coil was selected based on its high sensitivity, stability, and passive operation. Though an air core coil will have a lower voltage output compared to a magnetic core coil of the same dimensions, the air core was selected due to its linear response.

$$V = 0.5 \cdot 2\pi \cdot f \cdot n \cdot D^2 \cdot B \quad (1)$$

Equation 1 is the fundamental expression for induction coil output voltage in the presence of a changing magnetic field, according to Faraday's Law (Tumanski, 2007). In this equation, V is the voltage output, *f* is the frequency, *n* is the number of turns, *D* is the mean diameter of the coil, and *B* is the flux density to be measured.

The design parameters of the coil were chosen based on a desired 1 V output at 60 Hz based at an anticipated maximum flux density output of 10 G measured during experimental testing conducted with the Hall effect sensor. The outer diameter of the coil was chosen to be less than 10 cm to accommodate the size of the motor. The final design is a coil of 540 turns wound from 30 gauge magnet wire, and the length of the coil is 18 wire diameters. Once the parameters for the coil design were chosen, a spool for the coil was machined from Type II PVC. The wire was manually wound onto the coil, and the outer edge of the coil was bound to the spool with Kapton tape. The shape of the spool was designed so that the wire coil was held tangent to the motor case.

As with the small coil array, the RMS voltage output from the coil was initially surveyed at various locations and orientations on the motor. The final location was chosen that such that the crosstalk between phases at the output of the transducer was minimized. Although the output voltage from the coil was of a higher magnitude than the voltage from the small array, the relative change in voltage with respect to motor load was very similar for nearly all drive frequencies compared to the small coil array.

Parameter	Value
Motor Speed	1800, 2400, 2700, 3000, 3300, 3600 RPM
Generator Power Range	0-430 Watts (0-8 bulbs)
Step dwell time	30 seconds
Replicates	4x (216 total steps)
Transducers	Single Induction Coil Induction Coil Array Hall Effect IC
Data sampling rate	10 kHz
Motor Load Metric	Generator Output Power

Table 1. Stray Flux Transducer Characterization Study Parameters

3. TRANSDUCER CHARACTERIZATION

Preliminary sensor characterization revealed that the amplitude of the stray flux of the test motor varied not only with load, but with motor speed as well. Since the ultimate nonintrusive load monitoring system must operate under uncertain speed conditions, testing was conducted to characterize transducers across a wide range of loads *and* speeds. Outputs of the three stray flux transducers were characterized over the operational range of the motor test stand described in previous sections.

Table 1 provides the general parameters used for this set of experimental procedures. The operational range covers six motor speeds and nine power levels, where speed is automatically controlled by the LabVIEW application according to a user-defined profile and power is controlled manually by actuating individual light switches at the designated time. The system dwells at each load/speed parameter pair for 30 seconds before proceeding to the next step.

To provide an improved basis for statistics calculations, the speed and load profiles were replicated four times, and then randomized to develop the final profile. Input randomization during characterization and calibration minimizes the impact of interference, breaks up hysteresis errors, and ensures that each application of input values is independent from the previous. Generally, such random variation will more closely simulate the actual operating conditions ("Some Notes on Device Calibration," n.d.). Figure 4(a) illustrates the randomized motor speed parameters generated for the test, showing the first 1500 seconds for improved visualization.

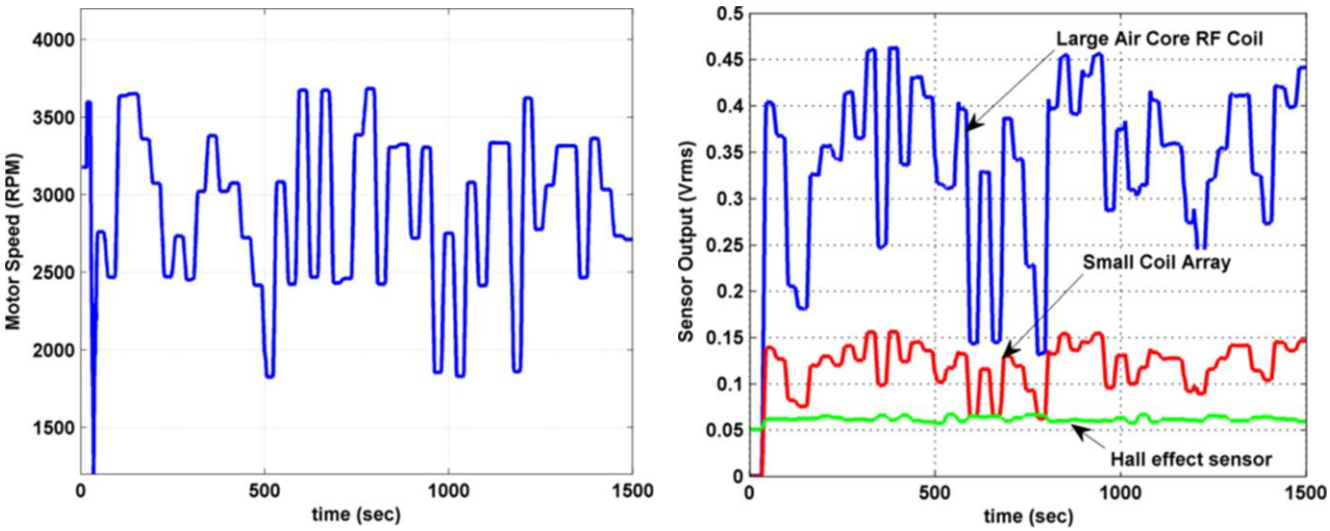

(a) Motor speed

(b) RMS voltage output of all three transducers

Figure 4. Representative time domain instrumentation data

As stated previously, generator output power was used as the means of monitoring motor load. It is notable that generator output voltage scales roughly with rotor speed, therefore the maximum output power is also speed dependent. The data presented in Figure 4(b) are the RMS values of the AC waveform for each sensor observed within one second windows of time, all showing correlation to the generator output power. The single and arrayed induction coil outputs trend inversely with power output, whereas the Hall effect sensor exhibits the opposite behavior. Relocating the Hall effect sensor around the same radius of the motor showed an inverse trend in the output, possibly due to the small size of the sensor compared to the size of the coil windings. The polarity of the outputs of the induction coils were not found to be sensitive to their location.

All of the signal streams were acquired at a rate of 10 kHz at one second intervals. The respective resulting 10,000 data points for each signal were then processed to provide a single RMS value for each one second time step, essentially reducing the data logging burden by several orders of magnitude. All subsequent analysis is performed using these RMS values. After the initial survey to validate that all transducer outputs were within expected intervals, a more rigorous analysis was performed to develop the sensor output trends over the speed and load operating envelope, discussed in the following section.

4. DISCUSSION

Figure 5 illustrates the dependence of sensor output on the applied motor speed and load (based on generator power) for the large coil (a), coil array (b), and Hall effect sensor (c). The colored dot markers indicate raw sensor data collected for each load and speed test point, with the marker colors indicating the different motor speeds. Figure 5(d) shows the relative response of the three sensors plotted on the same scale, highlighting the very high sensitivity of the large coil relative to the other two transducers. The raw data collected during the experiment described above was post-processed to provide straightforward visualization of the sensor response over the operating envelope, and to develop some statistical indicators of each sensor's ability to accurately monitor the motor load.

In all cases, the trend between the transducer output and output power is very linear and repeatable across motor speeds, as shown by the linear best-fit lines through the data. It is immediately evident, however, that transducer outputs vary with motor speed non-linearly. This fact warrants the measurement of speed by the nonintrusive sensor, in addition to stray flux. In the interest of maintaining the nonintrusive nature of sensor, the motor speed can be estimated by monitoring the fundamental frequency of the AC stray flux, instead of requiring a dedicated speed sensor. However, slip in induction motors under load may present an issue to the feasibility of this method, warranting further study.

As shown in Figure 5(d), collected data was interpolated to form a surface map that fully covers the motor's operating envelope. In practice, however, it is desirable to perform the load calibration with a minimum number of load and speed inputs given the likely limited ability to effect these changes in a plant environment. By inverting the axes so that motor power is on the z-axis, this data can be used to assemble a transfer function with two inputs (speed, RMS sensor output) that can be evaluated using inputs measured from a single coil mounted to the exterior of the motor.

Using the calibration maps established above, it is straightforward to determine how well the measured data fit

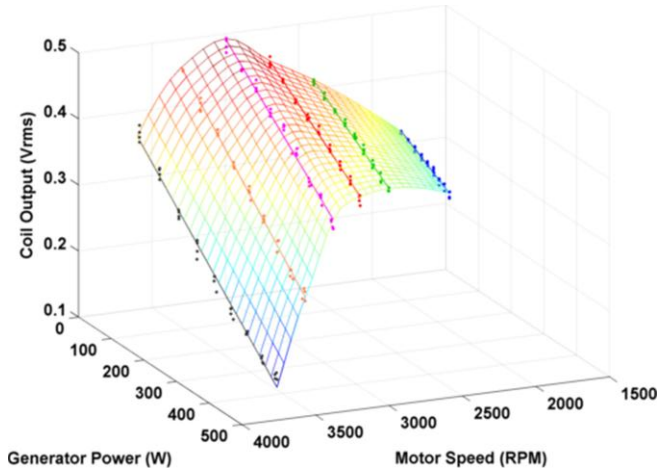

(a) Large coil output vs. motor speed, load

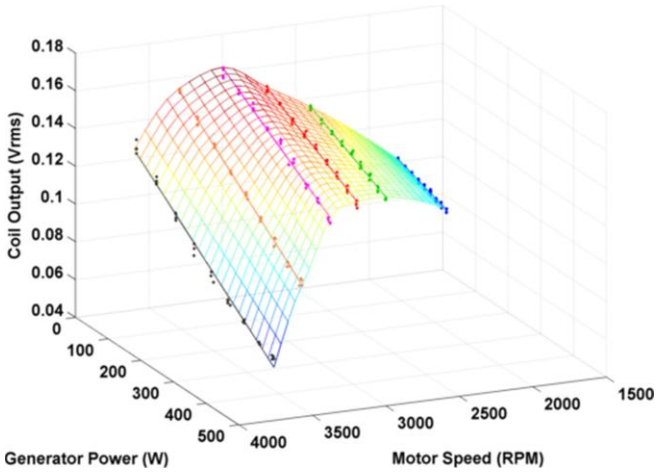

(b) Coil array output vs. motor speed, load

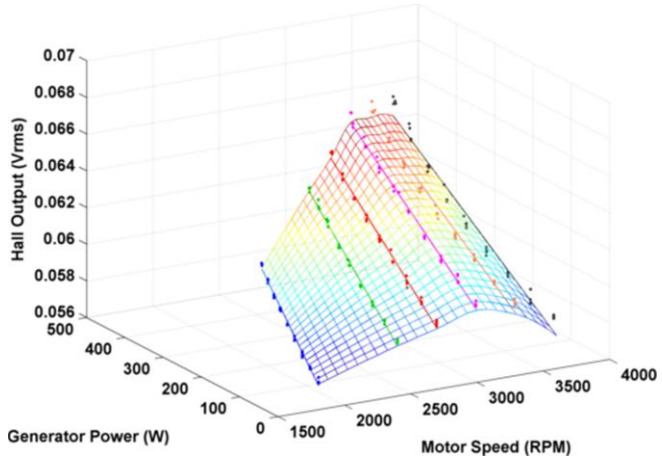

(c) Hall effect output vs. motor speed, load; axes reversed

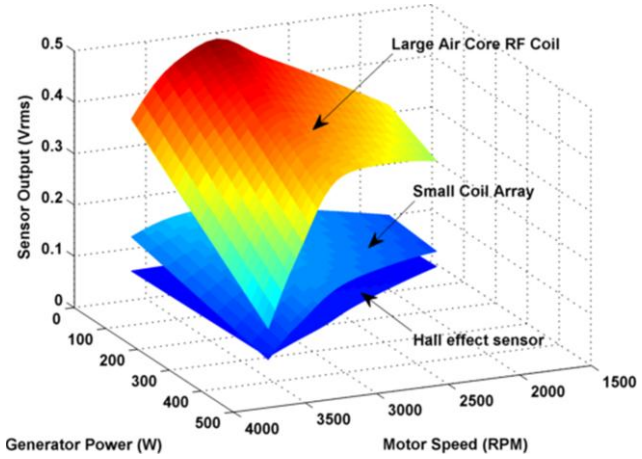

(d) Relative response of the three sensors

Figure 5. Dependence of sensor output on the applied motor speed and load

to this surface and thereby produce an indication of the accuracy of the load estimation given the spread in the sensor data. The difference between actual measured load and the model estimate was calculated, forming a residual error for each data point. Figure 6 presents the residual errors between the best-fit model and the measured data for each motor speed and load parameter pair, relative to the full scale load. The standard deviation of these residuals provides an indication of how well the data fit the calibration map. Assuming the standard deviation of these values as 1σ, the 95% confidence interval around the mean is established at ±2σ. In the case of the large coil, where σ = 3.3% full scale, this analysis indicates that the model can statistically determine the difference between any two load points with 95% confidence if their values differ by 6.6% full scale or greater (±2σ).

The Hall effect sensor performs rather well from the standpoint that it produces repeatable data, as indicated by reasonable standard deviations on the error, despite its very low sensitivity relative to the induction coils (10 vs. 400 mV full scale output). The coil array was less sensitive than the large coil and also produces a greater relative spread in the output, indicating a lower relative signal-to-noise ratio. From a sensor robustness standpoint, the large coil displays higher output, greater noise immunity, and the greatest precision among the three transducers.

Finally, Figure 7 illustrates the large coil response surfaces for two independent tests, revealing excellent agreement between the two runs. Using the large coil sensor response to compare two independent data collection runs provides a qualitative evaluation of repeatability of the proposed method.

5. Conclusions and Future Research

This work detailed the development of three transducers for stray flux detection as part of a system for nonintrusive load monitoring of rotating machinery. The large RF coil

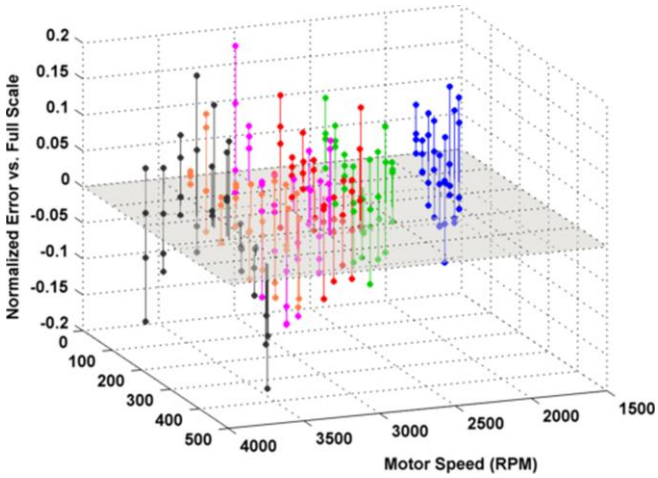

Figure 6. Normalized load estimation error for large air core RF coil, which was the best overall performer

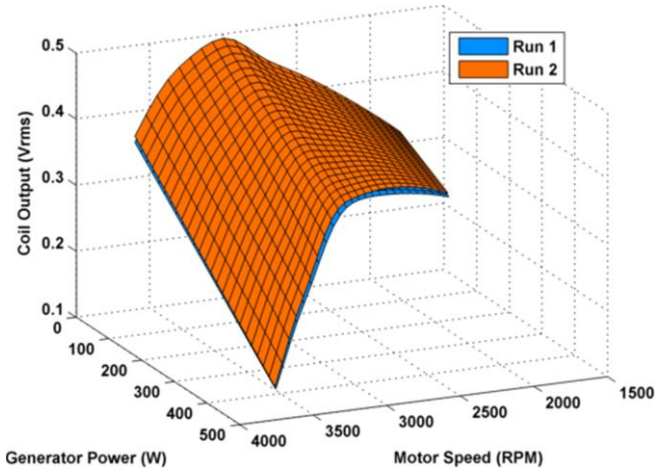

Figure 7. Comparing large coil response between two test runs as a preliminary assessment of repeatability

designed in this study was found to be the most effective transducer for measuring stray flux of an induction motor for the purpose of nonintrusively determining its mechanical load. Additionally, the carrier frequency of the same signal was found to be an accurate representation of the drive frequency of the motor. This suggests that a single transducer could be used to generate inputs to a two input (speed, RMS sensor output) transfer function to motor load. A statistical analysis of the transfer function showed that the calibration model can be used to determine the difference between any two load points with 95% confidence if their values differ by 6.6% full scale or greater ($\pm 2\sigma$). This demonstrates the validity of the approach to be used as a model that can predict mechanical motor load without any intrusive measurements.

Calibration of all studied transducers was determined to be necessary between placement and orientation cycles. However, in an active plant facility, placement and orientation of the nonintrusive sensor may be changed during maintenance or other activities. For practical purposes, it would be very convenient to develop a transducer or sensing method that would not require calibration between placement, allowing more flexible placement options. Further testing should be performed to measure the effects of changing position, orientation, and distance from the motor case on output voltage with respect to load.

Finally, further effort is warranted toward generalizing the method for application to a variety of machine types, including synchronous motor architectures. It remains to be determined whether the presented method would scale to larger motors, which may emit less stray flux due to higher efficiencies. Further experimental study will seek to identify common stray flux density signatures from different sizes of motors and motors based on various operating principles, such that these surfaces can be parameterized according to its expected characteristics, and require fewer calibration points to refine the calibration model once installed in the field. Determining similarities of the stray flux signatures emitted by various types of machines would facilitate the development of a parameterized model that could then be configured with motor specifications or a small number of calibration points, that would scale the model to fit the particular machine of interest. This and other development is needed to minimize the calibration effort needed to enable this approach to work in a practical setting.

ACKNOWLEDGEMENT

This material is based upon work supported by the United States Air Force under Contract No. FA9101-11-C-0032. Any opinions, findings and conclusions or recommendations expressed in this material are those of the author(s) and do not necessarily reflect the views of the United States Air Force.

REFERENCES

Adam, A. A., Gulez, K., & Koroglu, S. (2001). Stray magnetic field distributed around a PMSM. *Turk J Elec Eng & Comp Sci*, *19*(1).

Bin Lu, Habetler, T. G., & Harley, R. G. (2006). A survey of efficiency-estimation methods for in-service induction motors. *IEEE Transactions on Industry Applications*, *42*(4), 924–933. doi:10.1109/TIA.2006.876065

Determining Electric Motor Load And Efficiency. (n.d.). U.S. Department of Energy.

Some Notes on Device Calibration. (n.d.). Retrieved January 18, 2012, from http://www.iceweb.com.au/Test&Calibration/NoteDeviceCalibration.pdf

Tumanski, S. (2007). Induction Coil Sensors - A Review.pdf. *Meas. Sci. Technol.*, (18), R31–R46. doi:10.1088/0957-0233/18/3/R01